ACS Sustainable Chemistry & Engineering

Research Article

pubs.acs.org/journal/ascecg

Enhancing Thermomechanical Properties and Heat Distortion Resistance of Poly(L-lactide) with High Crystallinity under High Cooling Rate

Hai-Yan Yin,[†] Xin-Feng Wei,[†] Rui-Ying Bao,*[,†] Quan-Xiao Dong,[‡] Zheng-Ying Liu,[†] Wei Yang,*[,†] Bang-Hu Xie,[†] and Ming-Bo Yang[†]

[†]State Key Laboratory of Polymer Materials Engineering, College of Polymer Science and Engineering, Sichuan University, Chengdu 610065, Sichuan, People's Republic of China

[‡]Beijing Engineering Research Center of Architectural Functional Macromolecular Materials, Beijing Building Construction Research Institute, Beijing 100039, People's Republic of China

Supporting Information

ABSTRACT: In this work, a novel, effective and simple approach to largely improve the thermomechanical properties and heat distortion resistance of biodegradable poly(L-lactide) (PLLA) by using a new nucleating agent (NA), i.e., itself high-melting-point homocrystallites (*h*PLLA crystallites) is reported. Specially, *h*PLLA crystallites with a melting temperature (T_m) of 187 °C were introduced into the PLLA matrix with a lower T_m, i.e., 168 °C via simply melt blending at 170 °C which is between the T_ms of the two PLLAs. Nonisothermal and isothermal crystallization results reveal that *h*PLLA crystallite is an efficient nucleating agent for PLLA. Also, *h*PLLA crystallites show much more prominently promoting effect on the crystallization rate of PLLA in comparison with two widely reported NAs for PLLA, talc and stereocomplex crystallites. Most importantly, this promoting effect is still efficient at very high cooling rate, leading to a crystallinity of 39.1% at a cooling rate of 100 °C/min, which can help to obtain high-crystallinity PLLA products in conventional manufacturing processes. The optical microscopic observation reveals that the remarkable crystallization promotion can be attributed to the outstanding heterogeneous nucleation effect, as a result of both identical chemical constitution and lattice constitution between *h*PLLA crystallites and PLLA matrix. Further characterizations indicate that the enhancement of PLLA crystallinity by using such a new efficient NA can enhance the thermomechanical properties and heat distortion resistance of PLLA remarkably. For instance, at 80 °C (above T_g of PLLA), the elastic modulus increases by 60 times from 8 to 477 MPa with the incorporation of 5 wt % *h*PLLA.

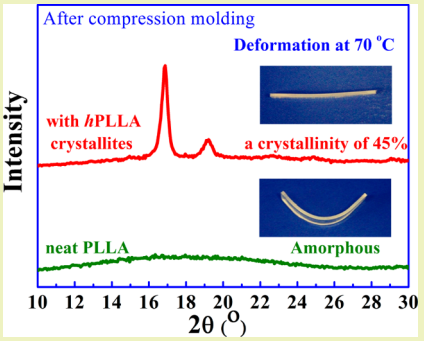

KEYWORDS: *Biodegradable polylactides, nucleating agent, high crystallinity, thermomechanical properties, heat distortion resistance*

INTRODUCTION

With the growing awareness of sustainability, poly(L-lactide) (PLLA), one of the most promising ecofriendly biopolymers, has exhibited vast appeal in the past decades due to its excellent performance in renewability, biodegradability and biocompatibility.[1−6] Although it is semicrystalline, PLLA is usually amorphous after processing owing to its extremely slow crystallization rate and fast cooling rate in conventional processing methods such as injection and compression molding.[7,8] Additionally, its glass transition temperature (T_g) is relatively low (in the range of 50−60 °C), leading to poor heat resistance of PLLA products, which even distorts during high-temperature sterilization before use. The enhancement on PLLA crystallinity has been regarded as one of the simplest and most practical approaches to improve its heat resistance performance.[9−12] For example, heat deflection temperature (HDT) and Vicat penetration temperature were increased for more than 30 and 100 °C, respectively, after amorphous samples were fully crystallized.[8] At the same time, other properties such as barrier property can also be improved by increasing the crystallinity of PLLA.[7,8,1314]

To tailor the crystallization of PLLA, nucleating agents (NAs) are usually employed. Various chemical/organic/mineral components, carbon fillers and stereocomplex (SC) crystallites formed between PLLA and poly(D-lactide) (PDLA) have been reported to be NAs for PLLA.[8,15−25] They can enhance the nucleation of PLLA by providing heterogeneous nucleation sites, and thus promote the crystallization kinetics. However, in previous reports, generally a relatively slow cooling rate, e.g., 10 °C/min or even less, was selected. In conventional manufacturing processes such as injection molding and compression molding, the polymer is typically cooled from its melt processing temperature down to mold temperature within seconds and thus the cooling rate is as high as 100 °C/min or

Received: December 4, 2014
Revised: March 4, 2015
Published: March 13, 2015

DOI: 10.1021/sc500783s
ACS Sustainable Chem. Eng. 2015, 3, 654−661

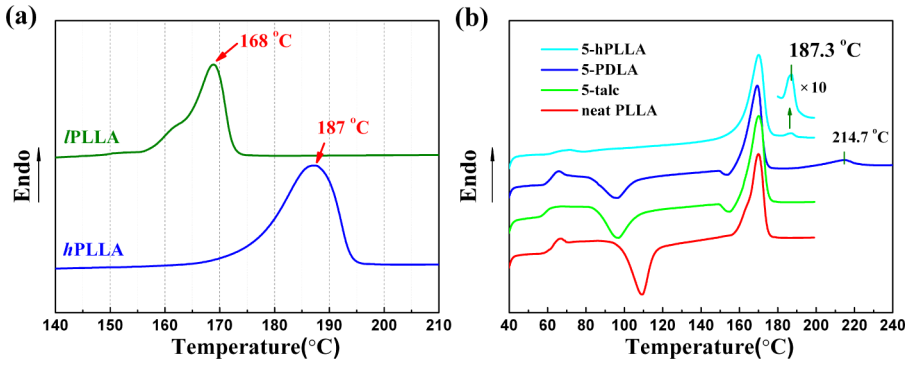

Figure 1. DSC melting curves at a rate of 10 °C/min of the two semicrystalline grade PLLAs (a) and the melt blended samples (b). 5-talc, 5-PDLA and 5-*h*PLLA represent samples of *l*PLLA melt blended with 5 wt % talc, PDLA and *h*PLLA, respectively.

even higher rather than 10 °C/min or less used in conventional thermal analysis.[7] So, whether these NAs can still enhance the crystallization of PLLA effectively during conventional manufacturing processes (under high cooling rates) is still questionable. Li and Huneault[7] reported that talc (5 wt %), one of the most common used NAs for PLLA,[8,15] can improve the crystallization enthalpy of PLLA to 40 J/g at a cooling rate of 10 °C/min, which reduced to only 18 J/g at cooling of 40 °C/min. In our previous work, with the incorporation of 1 wt % PDLA, which can complex with its enantiomeric PLLA to form SC crystallites, another efficient NA for PLLA,[16,26,27] the crystallinity of PLLA reached 40% at a cooling rate of 10 °C/min, while reduced to 5% at 40 °C/min.[28] These results show that it is still a great challenge to obtain high crystallinity PLLA products in conventional manufacturing processes with high cooling rates.

For this issue, the most direct way is to seek a more efficient NA for PLLA. Generally, NAs work following the epitaxial nucleation mechanism, i.e., crystallization occurs by epitaxial growth of polymer chains on NA surface, during which the interactions between polymer melt and NA surface and the lattice matching between polymer and NAs play key roles.[29] On the basis of the point of favorable interaction and lattice matching, in the present work, we came up with the idea of using high-melting-point crystallites of PLLA to accelerate the crystallization rate of PLLA. By using its own crystallites as a new NA source of PLLA, it can be predicted that there exist both identical chemical constitution and lattice constitution between NA and PLLA matrix, thus a high efficient NA and a high crystallinity PLLA may be achieved to improve the thermomechanical properties and heat resistance of PLLA.

In fact, the melting points of PLLA can be easily adjusted in a huge range from 120 to 200 °C by controlling the optical purity (i.e., the content of D-lactide isomers in PLLA chains), molecular weight and the crystallization conditions,[6,8,30] which was utilized delicately to achieve the reservation of a certain amount of high-temperature unmelt PLLA homocrystallites in the melt of PLLA matrix during processing in this work. The unmelted high-melting-point PLLA crystallites turn out to be an efficient nucleating agent for PLLA and can significantly accelerate the crystallization rate of PLLA under high cooling rates, which will show great value in conventional manufacturing processes and expand the applications of PLLA.

EXPERIMENTAL SECTION

Materials. Two semicrystalline grade PLLAs with different melting points were used. A PLLA resin (trade name 4032D) comprises about 2% D-units, with a weight-averaged molecular weight (M_w) of 2.1 × 10^5 g mol^{-1}, supplied by NatureWorks LLC (USA), was named as *l*PLLA. Another PLLA resin with a M_w of 5.7 × 10^5 g mol^{-1}, synthesized by ring-opening polymerization of L-lactide, supplied by Jinan Daigang Biomaterial Co., Ltd., was served as the high-melting-point PLLA (*h*PLLA), i.e., the nucleating agent source. The melting points of *l*PLLA and *h*PLLA are 168 and 187 °C, respectively (measured by differential scanning calorimetry (DSC) at a heating rate of 10 °C/min, see Figure 1a). The difference in the melting points for these two PLLA resins is as high as 19 °C so that a relatively broad processing temperature window for keeping the *h*PLLA crystallites unmelted can be utilized. PDLA with a M_w of 1.0 × 10^5 g mol^{-1}, synthesized by ring-opening polymerization of D-lactide, was kindly supplied by Professor Chen Xue-Si at the State Key Laboratory of Polymer Physics and Chemistry, China. Talc was purchased from Tuoyi Trade Co., Guangzhou (China).

Sample Preparation. The *h*PLLA powders were annealed in a vacuum oven at 120 °C for 3 h to induce a high degree of crystallinity (55.2%, calculated by its wide-angle X-ray diffraction result) and then were sieved through a 150 μm mesh to reduce the average grain size of the particles. Then 5 wt % of the refined *h*PLLA powders were compounded into molten *l*PLLA in a Haake internal mixer (Rheomix 600, Germany) at 40 rpm for 5 min at 170 °C, which is between the melting points of two selected PLLA resins. For comparison, 5 wt % of PDLA, and talc were also melt blended with *l*PLLA under the same conditions. Prior to blending, the resins and talc were vacuum-dried at 60 °C for 24 h. Neat *l*PLLA was also processed under the same conditions, also for comparison. The prepared samples were again dried at 60 °C for 6 h and then compression molded into bar-type samples with a size of 35 × 6 × 1 mm^3 on a hot-press at 175 °C and 10 MPa and then cooled on a cold-press at 90 °C and 10 MPa for 3 min. These compression-molded samples were used for the characterization of mechanical properties and heat resistance. In addition, films with a thickness of about 30 μm were also prepared by hot-pressing at 175 °C for optical microscopic observation.

Differential Scanning Calorimetry (DSC). The melting behaviors of the melt-blended specimens were investigated with DSC at a heating rate of 10 °C/min using a DSC Q20 (TA Instruments, USA). The nonisothermal and isothermal crystallization behaviors of neat PLLA and NA-nucleated samples were also recorded. Samples of around 8 mg were first heated to 180 °C at a rate of 100 °C/min and held for 3 min, then cooled to 30 °C at a rate of 2.5 °C/min to record the nonisothermal crystallization behavior. For isothermal crystallization, samples were also first held at 180 °C for 5 min and then cooled to the selected isothermal crystallization temperatures at the fastest cooling rate of this equipment (about 40 °C/min) to monitor the isothermal crystallization process. All these processes were carried out under nitrogen atmosphere.

To observe the crystallization behaviors of the samples under high cooling rate, Diamond DSC (PerkinElmer, USA), which can achieve a relatively high cooling rate, was employed. Samples were first heated to 180 °C at a rate of 100 °C/min and held for 3 min, then cooled to

DOI: 10.1021/sc500783s
ACS Sustainable Chem. Eng. 2015, 3, 654−661

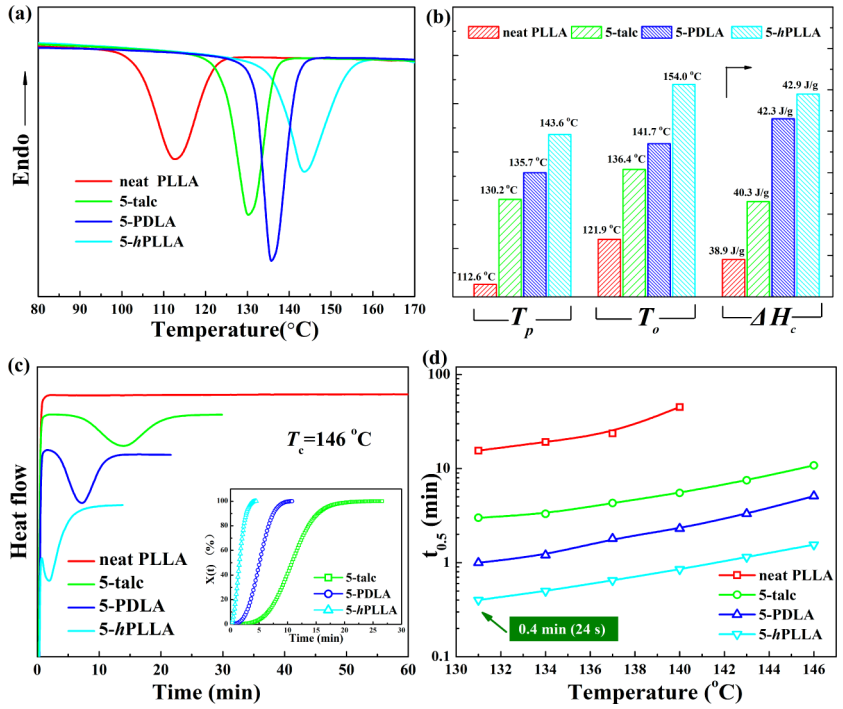

Figure 2. (a) DSC cooling curves of neat *l*PLLA and blended samples at a rate of 2.5 °C/min; (b) crystallization peak temperature (T_p), onset temperature (T_o) and crystallization enthalpy (ΔH_c) obtained from the cooling curves; (c) DSC heating flow as a function of time at isothermal crystallization temperatures of 146 °C and the inset displays the relative crystallinity as a function of time and (d) the half crystallization time ($t_{0.5}$) obtained at different crystallization temperatures from relative crystallinity of 50%.

30 °C at a relatively high cooling rate, i.e., 100 °C/min, and last reheated to 200 °C at a rate of 10 °C/min to record the melting behavior.

Polarizing Optical Microscopy (POM). The nucleation and crystalline morphologies of neat PLLA and NA-nucleated samples were observed using an Olympus BX51 polarizing optical microscopy (Olympus Co., Tokyo, Japan) equipped with a hot-stage (LINKAM THMS 600). The hot-pressed films of neat PLLA and its NA-nucleated samples, sandwiched between two cover glasses, were melted at 180 °C for 5 min, and then quickly cooled to 140 °C at a cooling rate of 50 °C/min for isothermal crystallization.

Wide-Angle X-ray Diffraction (WAXD). WAXD measurements of the compressed samples were carried out with a DX-1000 X-ray diffractometer (Dandong Fanyuan Instrument Co. LTD, China) using a Cu Kα radiation source (λ = 0.154 056 nm, 40 kV, 25 mA) in the scanning angle range of 2θ = 5−50° at a scan speed of 3°/min.

Dynamic Mechanical Analyzer (DMA). To explore the heat resistance and thermomechanical performance, dynamic mechanical properties of the compressed samples were studied by a dynamic mechanical analyzer (Q800, TA Instruments, USA) with a tensile mode at a strain of 0.08% and frequency of 1 Hz from 20 to 140 °C at a heating rate of 3 °C/min.

RESULTS AND DISCUSSION

Introduction of High-melting Point PLLA Crystallites. To confirm that *h*PLLA crystallites were not melted during processing, the melting behaviors of the samples were investigated by DSC. As displayed in Figure 1b, neat *l*PLLA exhibits only one melting peak at around 170 °C at the first heating scan, whereas the sample with 5 wt % *h*PLLA shows an additional independent melting peak at 187.3 °C, which is exactly around the melting point of *h*PLLA crystallites, as displayed in Figure 1a, indicating that *h*PLLA crystallites were not melted during processing and were successfully reserved. Besides, it is clear that only PLLA α-crystal diffraction peaks appear for the sample of 5-*h*PLLA in its WAXD curve, as presented in the Supporting Information, Figure S1, suggesting no other crystal forms were introduced into *l*PLLA with the addition of *h*PLLA. A tiny melting peak at 215 °C, corresponding to the melting point of SC crystallites, is observed for the sample with 5 wt % PDLA, confirming that with the incorporation of PDLA, SC crystallites were also introduced as proposed in our previous work.[31−33] The same conclusion can also be obtained in Figure S1 of the Supporting Information as the diffraction peaks of SC crystallites were detected for the sample of 5-PDLA. Here, what needs to be pointed out is that even though the same content (5 wt %) of *h*PLLA, PDLA and talc was added in *l*PLLA, the actual contents of *h*PLLA crystallites, SC crystallites and talc in the blends are different. In particular, the crystallinity of *h*PLLA powder is 55.2%, thus the content of *h*PLLA crystallites in its blend is 2.8% (=5% × 55.2%). By a WAXD method, a content of 7.3% was obtained for SC crystallites in the *l*PLLA/PDLA blend from its curve in Figure S1 of the Supporting Information. The content of talc does not change and is 5%.

Nonisothermal and Isothermal Crystallization Behaviors. Nonisothermal and isothermal crystallization behaviors of neat *l*PLLA and its NA nucleated samples were studied to reveal the promoting effect of the reserved *h*PLLA crystallites on the crystallization of PLLA in comparison with those of talc and SC crystallites. Before crystallization, all samples were kept for 3 min at 180 °C (above the melting point of *l*PLLA matrix but below that of *h*PLLA crystallites and SC crystallites) at which only homocrystallites of *l*PLLA were melted, and *h*PLLA crystallites and SC crystallites were reserved. To obtain the crystallization peak of neat *l*PLLA during nonisothermal crystallization, a slow cooling rate, i.e., 2.5 °C/min, was selected. As shown in Figure 2a, with the incorporation of talc,

DOI: 10.1021/sc500783s
ACS Sustainable Chem. Eng. 2015, 3, 654−661

the crystallization temperature (T_c) shifts to higher temperature compared to that of neat *l*PLLA due to its heterogeneous nucleating effect. A higher T_c is observed for the sample with SC crystallites compared to that of talc, revealing that SC crystallites show higher nucleation efficiency than talc. Most excitingly, the presence of *h*PLLA crystallites shifts the T_c to a much higher temperature and the improvement is significantly higher than that in the blend with either talc or SC crystallites, indicating that *h*PLLA crystallites can dramatically promote the crystallization of PLLA. Furthermore, as discussed above, the content of *h*PLLA crystallites in the blend is lower than those of SC crystallites and talc, thus it can be concluded that the promoting effect of the *h*PLLA crystallites on the crystallization of PLLA is even much more remarkable than talc and SC crystallites.

To compare the crystallization kinetics of the samples quantitatively, the crystallization onset temperature (T_o), peak temperature (T_p) and enthalpy (ΔH), three key parameters related to the nucleation characteristics, the overall crystallization kinetics and the degree of crystallinity, respectively, were displayed in Figure 2b. The crystallization enthalpy (ΔH_c) of these samples is normalized by eq 1:[33,34]

$$\Delta H_c = \frac{\Delta H'_c}{1 - iX\ (\%)} \times 100\% \qquad (1)$$

where ΔH_c and $\Delta H'_c$ are the normalized enthalpy of crystallization and actual enthalpy of crystallization, respectively; X (%) is the content of the NAs, i.e., 5% for all the nucleated samples; i, the correction coefficient, is 1 for *h*PLLA and talc nucleated samples assuming all the *l*PLLA molecules can form PLLA homocrystallites and 2 for the PDLA nucleated sample, considering only the remaining uncomplexed *l*PLLA molecules can form PLLA homocrystallites. All of these parameters show the maximum for the sample with *h*PLLA crystallites. Taking T_o as an example, T_o is 121.9 °C for neat *l*PLLA and increases to 136.4 and 141.7 °C, showing 14.5 and 19.8 °C shift, for sample with 5 wt % talc and PDLA, respectively. The T_o of the sample with *h*PLLA crystallites sharply increases to 154.0 °C, showing a 32.1 °C shift, which is 2.2 and 1.7 times that of the sample with talc and PDLA, respectively. These results clearly show that (1) *h*PLLA crystallites can act as a high-efficiency NA for PLLA and accelerate the crystallization rate of PLLA remarkably; (2) the promoting effect of the *h*PLLA crystallites on the crystallization of PLLA is much more prominent than common NAs, i.e., talc and SC crystallites.

The excellent promoting effect of *h*PLLA crystallites on the crystallization of PLLA can be confirmed by isothermal crystallization. As shown in Figure 2c, at T_c = 146 °C, no heating flow peak is observed for neat *l*PLLA in a period as long as 60 min. However, obvious heating flow peaks are seen for the blends. Moreover, the peak position in the exothermic heating flow curves appears at a much shorter time for the sample with *h*PLLA crystallites compared to those of the samples with SC crystallites or talc. These results attested the much more remarkable crystallization accelerating effect of *h*PLLA crystallites than those of talc and SC crystallites.

The crystallization accelerating effect can be demonstrated more directly by the changes of half crystallization time ($t_{0.5}$), the time required to achieve half of the final crystallinity, which is a key parameter to characterize the overall crystallization kinetics. Neat *l*PLLA exhibits a $t_{0.5}$ above 10 min at these investigated T_c, whereas with the introduction of talc or PDLA, $t_{0.5}$ sharply decreased, and with the reservation of *h*PLLA crystallites, $t_{0.5}$ further decreases by 1−2 orders of magnitude compared with that of neat *l*PLLA. Taking the case of T_c = 131 °C as an example, $t_{0.5}$ drops to only 0.4 min, less than 1 min, for the sample with *h*PLLA crystallites, showing the overall crystallization rate (referring to $1/t_{0.5}$) increase of 37.5, 7.5 and 2.5 times in comparison with that of neat *l*PLLA, the samples with talc and SC crystallites, respectively.

For pure PLLA, the maximum crystallization rate, or the minimum $t_{0.5}$, was reached in the temperature range of 105−110 °C, at which the lowest reported $t_{0.5}$ was in the 2−3 min range.[8] However, at 131 °C, $t_{0.5}$ has already reduced to 0.4 min (24 s) with the reservation of *h*PLLA crystallites. So, such a short crystallization time is expected to match much better with the short cooling time, i.e., fast cooling rate, during conventional manufacturing processes and high-crystallinity PLLA products can be expected to be obtained by this novel NA, *h*PLLA crystallites.

Nucleation and Crystalline Morphologies during Isothermal Crystallization. To understand the excellent promoting effect of *h*PLLA crystallites on crystallization of PLLA, the nucleation and crystalline morphologies of neat *l*PLLA and its NA nucleated samples were investigated by POM observation. As shown in Figure 3, the presence of NAs

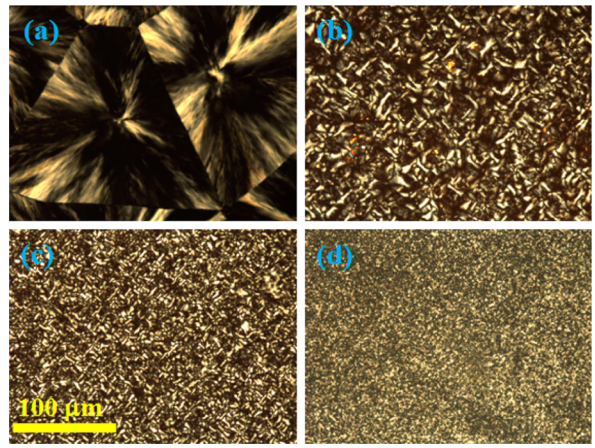

Figure 3. Spherulitic morphology of neat *l*PLLA (a) and the samples with 5 wt % talc (b), PDLA (c), and *h*PLLA (d) after isothermal crystallization at 140 °C.

results in the formation of a mass of small-sized spherulites. Moreover, as expected, the sample with *h*PLLA crystallites shows much more and smaller spherulites, i.e., a larger nucleation density, compared with the samples with SC crystallites and talc. These results clearly demonstrate that the nucleation ability of *h*PLLA crystallite is much more remarkable than the common NAs, i.e., talc and SC crystallites. As a result, its outstanding nucleation effect contributes to the significant promotion on crystallization rate of PLLA.

It is well-known that the unmelted crystallites or nuclei during the melting processing can enhance the nucleation process largely, which was defined as the self-nucleation effect or self-seeding.[35] Self-nucleation is considered to be an ideal case for polymer nucleation as both of the molecular interactions and lattice matching between the polymer melt and the nucleating surface are optimal because of identical chemical constituency and crystal lattice.[33,35−37] Here, the

DOI: 10.1021/sc500783s
ACS Sustainable Chem. Eng. 2015, 3, 654−661

unmelted crystallites, i.e., self-nuclei, are introduced delicately through the addition of high melting point PLLA crystallites rather than by melting the matrix partly, which is common adopted in the self-nucleation experiment. Thus, using PLLA itself crystallites, i.e., *h*PLLA crystallites, as NA for PLLA should also follows the self-nucleation mechanism and results in the outstanding nucleation effect.

Crystallization under High Cooling Rate. To check if *h*PLLA crystallites can still enhance the crystallization of PLLA under higher cooling rate effectively, the crystallization behaviors of the samples cooled from 180 °C at a relatively high cooling rate, i.e., 100 °C/min, were investigated by a PerkinElmer Diamond DSC instrument. The crystallinity (X_c) of these samples is calculated using eq 2:[38,39]

$$X_c = \frac{\Delta H_m - \Delta H_{cc}}{(1 - iX\ (\%))\Delta H^\circ} \times 100\% \quad (2)$$

where ΔH_m and ΔH_{cc} are the enthalpy of melting and cold crystallization of *l*PLLA, respectively; ΔH^0 is the melting enthalpy of 100% crystallized PLLA, i.e., 93 J g^{-1}; X (%) is the content of the NAs, i.e., 5% for all the nucleated samples; *i*, the correction coefficient, is 1 for *h*PLLA and talc nucleated samples assuming all the *l*PLLA molecules can form PLLA homocrystallites, and is 2 for the PDLA nucleated sample considering only the remaining uncomplexed *l*PLLA molecules can form PLLA homocrystallites.

As shown in Figure 4, a cold crystallization peak can be observed from the heating curves of neat *l*PLLA and the

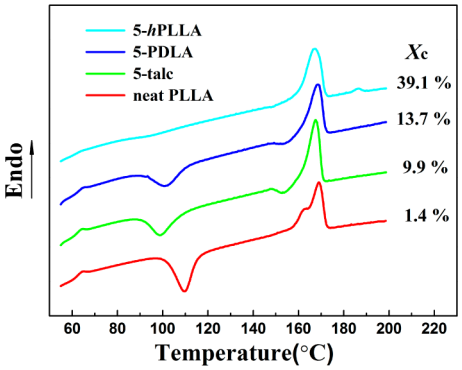

Figure 4. DSC melting curves at a heating rate of 10 °C/min of the samples cooled from 180 °C at a cooling rate of 100 °C/min.

samples with talc or SC crystallites, but disappears for the sample with *h*PLLA crystallites, revealing the incomplete crystallization for neat *l*PLLA, talc or SC crystallites nucleated samples and complete crystallization for *h*PLLA crystallites nucleated sample. The crystallinity of 9.9% and 13.7% is obtained for the sample with talc or SC crystallites, respectively, whereas the crystallinity is as high as 39.1% for the sample with *h*PLLA crystallites. These results indicate that the crystallization promoting effect of talc and SC crystallites on PLLA is limited at a high cooling rate, while *h*PLLA crystallites are still effective in accelerating the crystallization at such a high cooling rate of 100 °C/min. As a consequence, using *h*PLLA crystallites as NA for PLLA is more conducive to obtain PLLA products with high crystallinity under conventional process during which a relatively high cooling rate operates.

Thermomechanical Properties and Heat Distortion Resistance. Based on the discussion above, it is clear that *h*PLLA crystallite is a novel NA for PLLA and it is still efficient under a high cooling rate. Here, these samples were compressed into bar-type, during which they experienced a conventional processing method actually. To check the crystallization of these compressed samples, WAXD and DSC were employed, and the results are displayed in Figure 5a,b.

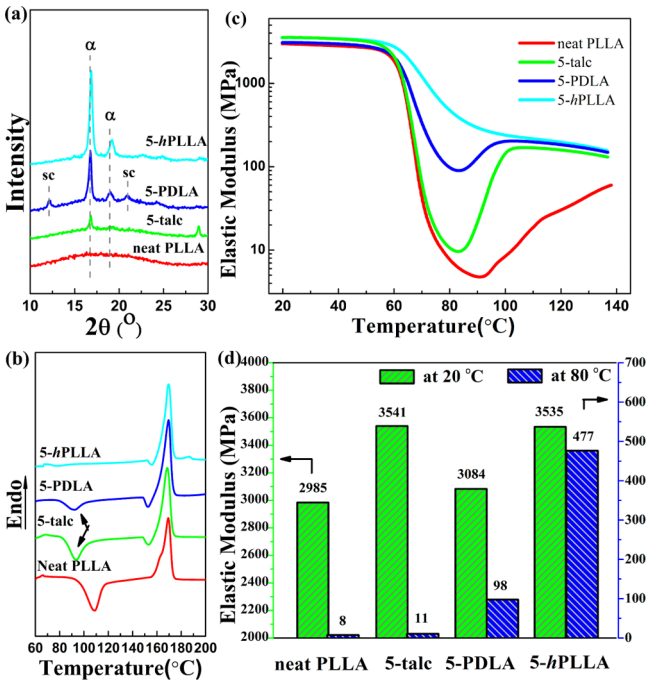

Figure 5. WAXD patterns (a), DSC heating curves (b), temperature dependence of elastic modulus (c), and elastic modulus at 20 and 80 °C of the compressed samples for neat PLLA and its blends (d).

In Figure 5a, no diffraction peaks exhibit for neat *l*PLLA, revealing that it is almost amorphous due to its extremely slow crystallization rate. Whereas the diffraction peaks at 2θ values of 16.7° and 19.0°, which correspond to the (200) and/or (110), and (203) planes of PLLA crystals in α-phase,[40] respectively, are observed for these NA nucleated samples. The intensity of these diffraction peaks is much stronger for *h*PLLA crystallites nucleated sample than that of talc or SC crystallites nucleated sample. In Figure 5b, a cold crystallization peak can be observed from the heating curves of neat *l*PLLA and the samples with talc or SC crystallites, but disappears for the sample with *h*PLLA crystallites, which agrees well with the results of WAXD. In addition, the crystallinities of these samples were obtained by both WAXD and DSC methods, and were presented in Table 1. A relatively high crystallinity of

Table 1. Degree of Crystallinity (X_c) of These Compressed Samples Obtained by WAXD and the Degree of the Normalized Crystallinity (X_c) of *l*PLLA by DSC

samples	neat *l*PLLA	5-talc	5-PDLA	5-*h*PLLA
X_c (%)[a]	lower than 1%	7.4	30.3[c]	45.4
X_c (%)[b]	4.8	11.8	29.4	39.4

[a]Obtained from WAXD results in Figure 5a. [b]Obtained from DSC results in Figure 5b and normalized by eq 2. [c]Including the crystallinity of SC crystallites (7.3%), which correspond to the diffraction peaks at 2θ values of 11.8° and 20.6° in the curve for sample of 5-PDLA in Figure 5a.

DOI: 10.1021/sc500783s
ACS Sustainable Chem. Eng. 2015, 3, 654−661

45.4% by WAXD and 39.4% by DSC is obtained for the *h*PLLA crystallites nucleated sample, respectively, revealing that with the incorporation of *h*PLLA crystallites into PLLA matrix a high crystallinity can be obtained during such a conventional processing method. Here, what needs to be pointed out is that the *h*PLLA crystallites show the same WAXD diffraction peaks with *l*PLLA matrix, which also contributes to the overall crystallinity of the *h*PLLA crystallites nucleated sample in the WAXD method, whereas from the DSC curve, the melting peaks of *l*PLLA crystallites and *h*PLLA crystallites can be easily separated and the melting enthalpy of *h*PLLA was subtracted.

DMA was used to study the effect of such a high crystallinity on the thermomechanical properties of PLLA. Figure 5c presents the temperature dependence of elastic modulus of these compressed samples. As shown, the elastic modulus is almost constant below T_g (60 °C, obtaining from their tan δ curves) and starts to drop at around T_g. However, the *h*PLLA crystallites nucleated sample shows much less decrease and higher elastic modulus than those of neat *l*PLLA and talc or SC crystallites nucleated samples. The modulus for neat *l*PLLA and talc or SC crystallites nucleated samples increase again around 90 °C, which results from the cold crystallization of the crystallizable free amorphous region of PLLA.

Specially, the elastic modulus at 20 and 80 °C of neat *l*PLLA and NA nucleated samples was obtained and compared in Figure 5d. At 20 °C, the addition of 5 wt % *h*PLLA, which greatly improves the crystallinity of the PLLA matrix, improves the elastic modulus of neat *l*PLLA by 18% from 2985 to 3535 MPa, revealing the enhancement on PLLA crystallization by using such a new efficient NA can enhance the mechanical properties of PLLA. The addition of 5 wt % talc shows a similar reinforcement effect. At 80 °C, the modulus increases by 60 times from 8 to 477 MPa with the incorporation of 5 wt % *h*PLLA. However, at 80 °C, the modulus of talc and SC crystallites nucleated samples is 11 and 98 MPa, respectively, much less than that of *h*PLLA crystallites nucleated sample. This means the enhancement on the thermomechanical properties of PLLA by using *h*PLLA crystallites is more effective than those of talc and SC crystallites, which contributes to the heat resistance of PLLA.

To illustrate directly how the heat resistance of NA nucleated PLLA samples is improved at high temperatures, the straight specimens obtained from compression molding were set in a fixture with a 50 g weight hung in the middle of the samples along the length direction, as shown in the schematic illustration in Figure 6. Then these specimens were placed into an oven at 70 °C (above T_g) for 5 min to observe the deformation of PLLA specimens upon loading. After this test, the deformation of these observational samples was recorded by taking photos and the photos were also displayed in Figure 6. It was observed that both neat *l*PLLA and talc and SC crystallites nucleated samples experienced serious deformation in no more than 2 min (as shown in Figure 6) and failed in supporting the load, resulting in dropping down with the weight. However, the *h*PLLA crystallites nucleated sample did not appear any visible deformation as long as 5 min, showing an excellent heat distortion resistance performance.

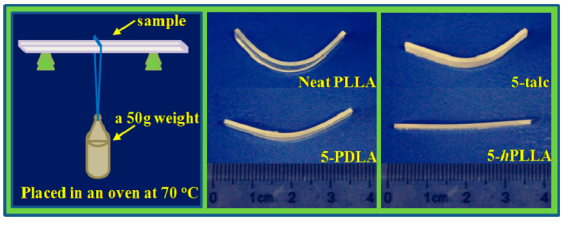

Figure 6. Schematic illustration of the designed heat distortion resistance test and the photos of these samples after the test.

As known, amorphous polymer materials transform from glass state to rubber state around the T_g, during which the molecular chain segments achieve the energy for moving and the mechanical properties such as modulus and strength decline sharply. However, for a crystallized polymer matrix, a large amount of chain segments are frozen in the crystallites and lose the ability of movement during glass transition. Furthermore, these crystallites can still reinforce the matrix above the T_g. As a result, PLLA with a high crystallinity achieved by nucleating of *h*PLLA crsytallites shows a high elastic modulus above the T_g and an excellent heat resistance. What should be pointed out is that polymer materials cannot be 100% crystalline, so during glass transition there still exists α-relaxation of amorphous structure and the mechanical properties will also decrease (seeing the modulus drop of *h*PLLA crsytallites nucleated sample). However, compared to amorphous matrix, such a decrease is much less and results in reinforcing the matrix above the T_g.

At last, it should be pointed out that high-melting-point crystallites of PLLA can be regarded as a green NA for PLLA and the utilization of such a green NA will not lose the excellent performance in biodegradability and biocompatibility of PLLA.

CONCLUSION

In the present work, a novel and effective approach to achieve high crystallinity PLLA by utilizing high-melting-point PLLA homocrystallites is presented. The *h*PLLA crystallites were introduced into PLLA matrix via melt blending at a processing temperature between the melting points of the selected PLLA resins. The nonisothermal and isothermal results reveal that *h*PLLA crystallites can accelerate PLLA crystallization rate more remarkably than common nucleating agents including talc and SC crystallites. In addition, the promoting effect of *h*PLLA crystallites can also be effective at a high cooling rate, which is conducive to obtain PLLA products with high crystallinity under conventional processes with high cooling rates. Such enhancement on PLLA crystallinity increased the elastic modulus by 60 times at 80 °C, contributing to improvement in thermomechanical properties and heat distortion resistance for PLLA material. The enhancement of the thermomechanical properties above the T_g can extend the application of PLLA, particularly for products exposed to high temperatures. In addition, this work also provides a new way to tailor the crystallization of polymers with slow crystallization rates in conventional processing techniques.

ASSOCIATED CONTENT

Supporting Information

WAXD profiles of the *l*PLLA samples containing talc, PDLA and *h*PLLA, melt blended at at 170 °C. This material is available free of charge via the Internet at http://pubs.acs.org/.

AUTHOR INFORMATION

Corresponding Authors

*W. Yang. Tel/Fax: + 86 28 8546 0130. E-mail: weiyang@scu.edu.cn.

DOI: 10.1021/sc500783s
ACS Sustainable Chem. Eng. 2015, 3, 654−661

*R.-Y. Bao. Tel/Fax: + 86 28 8546 0130. E-mail: baoruiying2005@126.com.

Notes

The authors declare no competing financial interest.

■ ACKNOWLEDGMENTS

This work was supported by the National Natural Science Foundation of China (NNSFC Grants 51422305, 21374065 and 51421061), Major State Basic Research Development Program of China (973 program) (2012CB025902) and the Innovation Team Program of Science & Technology Department of Sichuan Province (Grant 2014TD0002) and State Key Laboratory of Polymer Materials Engineering (Grant No. sklpme2014-2-02).

■ REFERENCES

(1) Wagner, A.; Poursorkhabi, V.; Mohanty, A. K.; Misra, M. Analysis of porous electrospun fibers from poly(L-lactic acid)/poly(3-hydroxybutyrate-*co*-3-hydroxyvalerate) blends. *ACS Sustainable Chem. Eng.* **2014**, *2* (8), 1976−1982.

(2) Liu, H.; Zhang, J. Research progress in toughening modification of poly(lactic acid). *J. Polym. Sci., Part B: Polym. Phys.* **2011**, *49* (15), 1051−1083.

(3) Tsujimoto, T.; Uyama, H. Full biobased polymeric material from plant oil and poly(lactic acid) with a shape memory property. *ACS Sustainable Chem. Eng.* **2014**, *2* (8), 2057−2062.

(4) Sun, Y.; He, C. Biodegradable "core-shell" rubber nanoparticles and their toughening of poly(lactides). *Macromolecules* **2013**, *46* (24), 9625−9633.

(5) Zhang, Y.; Xu, H.; Yang, J.; Chen, S.; Ding, Y.; Wang, Z. Significantly accelerated spherulitic growth rates for semicrystalline polymers through the layer-by-layer film method. *J. Phys. Chem. C* **2013**, *117* (11), 5882−5893.

(6) Shao, J.; Sun, J.; Bian, X.; Cui, Y.; Zhou, Y.; Li, G.; Chen, X. Modified PLA homochiral crystallites facilitated by the confinement of PLA stereocomplexes. *Macromolecules* **2013**, *46* (17), 6963−6971.

(7) Li, H. B.; Huneault, M. A. Effect of nucleation and plasticization on the crystallization of poly(lactic acid). *Polymer* **2007**, *48* (23), 6855−6866.

(8) Saeidlou, S.; Huneault, M. A.; Li, H.; Park, C. B. Poly(lactic acid) crystallization. *Prog. Polym. Sci.* **2012**, *37* (12), 1657−1677.

(9) Srithep, Y.; Nealey, P.; Turng, L. S. Effects of annealing time and temperature on the crystallinity and heat resistance behavior of injection-molded poly(lactic acid). *Polym. Eng. Sci.* **2013**, *53* (3), 580−588.

(10) Suryanegara, L.; Nakagaito, A. N.; Yano, H. The effect of crystallization of PLA on the thermal and mechanical properties of microfibrillated cellulose-reinforced PLA composites. *Compos. Sci. Technol.* **2009**, *69* (7−8), 1187−1192.

(11) Zhong, Y.; Fang, H.; Zhang, Y.; Wang, Z.; Yang, J.; Wang, Z. Rheologically determined critical shear rates for shear-induced nucleation rate enhancements of poly(lactic acid). *ACS Sustainable Chem. Eng.* **2013**, *1* (6), 663−672.

(12) Bao, R.-Y.; Yang, W.; Wei, X.-F.; Xie, B.-H.; Yang, M.-B. Enhanced formation of stereocomplex crystallites of high molecular weight poly(L-lactide)/poly(D-lactide) blends from melt by using poly(ethylene glycol). *ACS Sustainable Chem. Eng.* **2014**, *2* (10), 2301−2309.

(13) Liu, G.; Zhang, X.; Wang, D. Tailoring crystallization: Towards high-performance poly(lactic acid). *Adv. Mater.* **2014**, *26* (40), 6905−6911.

(14) Pan, P.; Inoue, Y. Polymorphism and isomorphism in biodegradable polyesters. *Prog. Polym. Sci.* **2009**, *34* (7), 605−640.

(15) Tsuji, H.; Takai, H.; Fukuda, N.; Takikawa, H. Non-isothermal crystallization behavior of poly(L-lactic acid) in the presence of various additives. *Macromol. Mater. Eng.* **2006**, *291* (4), 325−335.

(16) Tsuji, H.; Takai, H.; Saha, S. K. Isothermal and non-isothermal crystallization behavior of poly(L-lactic acid): Effects of stereocomplex as nucleating agent. *Polymer* **2006**, *47* (11), 3826−3837.

(17) Xu, Z.; Niu, Y.; Yang, L.; Xie, W.; Li, H.; Gan, Z.; Wang, Z. Morphology, rheology and crystallization behavior of polylactide composites prepared through addition of five-armed star polylactide grafted multiwalled carbon nanotubes. *Polymer* **2010**, *51* (3), 730−737.

(18) Sun, J.; Yu, H.; Zhuang, X.; Chen, X.; Jing, X. Crystallization behavior of asymmetric PLLA/PDLA blends. *J. Phys. Chem. B* **2011**, *115* (12), 2864−2869.

(19) Krikorian, V.; Pochan, D. J. Unusual crystallization behavior of organoclay reinforced poly(L-lactic acid) nanocomposites. *Macromolecules* **2004**, *37* (17), 6480−6491.

(20) Nam, J. Y.; Sinha Ray, S.; Okamoto, M. Crystallization behavior and morphology of biodegradable polylactide/layered silicate nanocomposite. *Macromolecules* **2003**, *36* (19), 7126−7131.

(21) Martínez-Tong, D. E.; Vanroy, B.; Wübbenhorst, M.; Nogales, A.; Napolitano, S. Crystallization of poly(L-lactide) confined in ultrathin films: Competition between finite size effects and irreversible chain adsorption. *Macromolecules* **2014**, *47* (7), 2354−2360.

(22) Song, P.; Chen, G.; Wei, Z.; Chang, Y.; Zhang, W.; Liang, J. Rapid crystallization of poly(L-lactic acid) induced by a nanoscaled zinc citrate complex as nucleating agent. *Polymer* **2012**, *53* (19), 4300−4309.

(23) Mary Michell, R.; Mueller, A. J.; Boschetti-de-Fierro, A.; Fierro, D.; Lison, V.; Raquez, J.-M.; Dubois, P. Novel poly(ester-urethane)s based on polylactide: From reactive extrusion to crystallization and thermal properties. *Polymer* **2012**, *53* (25), 5657−5665.

(24) Qian, X.; Xiuqin, Z.; Xia, D.; Guoming, L.; Dujin, W. Low-molecular weight aliphatic amides as nucleating agents for poly(L-lactic acid): Conformation variation induced crystallization enhancement. *Polymer* **2012**, *53* (11), 2306−2314.

(25) Pei, A.; Zhou, Q.; Berglund, L. A. Functionalized cellulose nanocrystals as biobased nucleation agents in poly(L-lactide)-(PLLA)—Crystallization and mechanical property effects. *Compos. Sci. Technol.* **2010**, *70* (5), 815−821.

(26) Rahman, N.; Kawai, T.; Matsuba, G.; Nishida, K.; Kanaya, T.; Watanabe, H.; Okamoto, H.; Kato, M.; Usuki, A.; Matsuda, M.; Nakajima, K.; Honma, N. Effect of polylactide stereocomplex on the crystallization behavior of poly(L-lactic acid). *Macromolecules* **2009**, *42* (13), 4739−4745.

(27) Sun, Y.; He, C. Synthesis and stereocomplex crystallization of poly(lactide)-graphene oxide nanocomposites. *ACS Macro Lett.* **2012**, *1* (6), 709−713.

(28) Wei, X.-F.; Bao, R.-Y.; Cao, Z.-Q.; Zhang, L.-Q.; Liu, Z.-Y.; Yang, W.; Xie, B.-H.; Yang, M.-B. Greatly accelerated crystallization of poly(lactic acid): Cooperative effect of stereocomplex crystallites and polyethylene glycol. *Colloid Polym. Sci.* **2014**, *292* (1), 163−172.

(29) Li, H.; Yan, S. Surface-induced polymer crystallization and the resultant structures and morphologies. *Macromolecules* **2011**, *44* (3), 417−428.

(30) Tsuji, H.; Ikada, Y. Crystallization from the melt of poly(lactide)s with different optical purities and their blends. *Macromol. Chem. Phys.* **1996**, *197* (10), 3483−3499.

(31) Bao, R.-Y.; Yang, W.; Jiang, W.-R.; Liu, Z.-Y.; Xie, B.-H.; Yang, M.-B.; Fu, Q. Stereocomplex formation of high-molecular-weight polylactide: A low temperature approach. *Polymer* **2012**, *53* (24), 5449−5454.

(32) Bao, R.-Y.; Yang, W.; Jiang, W.-R.; Liu, Z.-Y.; Xie, B.-H.; Yang, M.-B. Polymorphism of racemic poly(L-lactide)/poly(D-lactide) blend: Effect of melt and cold crystallization. *J. Phys. Chem. B* **2013**, *117* (13), 3667−3674.

(33) Wei, X.-F.; Bao, R.-Y.; Cao, Z.-Q.; Yang, W.; Xie, B.-H.; Yang, M.-B. Stereocomplex crystallite network in asymmetric PLLA/PDLA blends: Formation, structure, and confining effect on the crystallization rate of homocrystallites. *Macromolecules* **2014**, *47* (4), 1439−1448.

(34) Narita, J.; Katagiri, M.; Tsuji, H. Highly enhanced accelerating effect of melt-recrystallized stereocomplex crystallites on poly(L-lactic

DOI: 10.1021/sc500783s
ACS Sustainable Chem. Eng. 2015, 3, 654−661

acid) crystallization, 2—Effects of poly(D-lactic acid) concentration. *Macromol. Mater. Eng.* **2013**, *298* (3), 270−282.
(35) Fillon, B.; Wittmann, J.; Lotz, B.; Thierry, A. Self-nucleation and recrystallization of isotactic polypropylene (α phase) investigated by differential scanning calorimetry. *J. Polym. Sci. Polym. Phys.* **1993**, *31* (10), 1383−1393.
(36) Fillon, B.; Thierry, A.; Lotz, B.; Wittmann, J. Efficiency scale for polymer nucleating agents. *J. Therm. Anal. Calorim.* **1994**, *42* (4), 721−731.
(37) Schmidt, S. C.; Hillmyer, M. A. Polylactide stereocomplex crystallites as nucleating agents for isotactic polylactide. *J. Polym. Sci., Part B: Polym. Phys.* **2001**, *39* (3), 300−313.
(38) Harris, A. M.; Lee, E. C. Improving mechanical performance of injection molded PLA by controlling crystallinity. *J. Appl. Polym. Sci.* **2008**, *107* (4), 2246−2255.
(39) Na, B.; Wang, K.; Zhang, Q.; Du, R.; Fu, Q. Tensile properties in the oriented blends of high-density polyethylene and isotactic polypropylene obtained by dynamic packing injection molding. *Polymer* **2005**, *46* (9), 3190−3198.
(40) Hoogsteen, W.; Postema, A.; Pennings, A.; Ten Brinke, G.; Zugenmaier, P. Crystal structure, conformation and morphology of solution-spun poly(L-lactide) fibers. *Macromolecules* **1990**, *23* (2), 634−642.

DOI: 10.1021/sc500783s
ACS Sustainable Chem. Eng. 2015, 3, 654−661